Desalination and Water Treatment 317 (2024) 100145

Contents lists available at ScienceDirect

Desalination and Water Treatment

journal homepage: www.sciencedirect.com/journal/desalination-and-water-treatment/

Membrane distillation of saline feeds and produced water: A comparative study of an air-gap and vacuum-driven modules

Hussain Al-Sairfi[a,*], M.Z.A. Koshuriyan[b], Mansour Ahmed[a]

[a] Kuwait Institute for Scientific Research, P. O. Box: 24885, 13109 Safat, Kuwait
[b] Department of Mathematics, University of York, Heslington, York YO10 5DD, United Kingdom

ARTICLE INFO

Keywords:
Air gap membrane distillation
Vacuum membrane distillation
Arabian Gulf seawater
Oil field-produced water
Vacuum space
Permeate flux

ABSTRACT

Air gap membrane distillation (AGMD) and vacuum membrane distillation (VMD) are two membrane-based desalination processes that utilize temperature differences to generate water vapor for purification. This study evaluated the viability of both processes for treating different types of saline water, such as Arabian Gulf seawater and oil field-produced water. Factors such as feed temperature, feed concentration, recirculation flow rate, air gap, and vacuum space depth were investigated to understand their impact on permeate flux in AGMD and VMD configurations. The results showed that AGMD achieved higher permeate flux at lower feed concentrations, while VMD performed better at higher concentrations. Increasing the feed temperature led to increased permeate flux in both configurations, with AGMD showing a greater increase. Results also indicated that lower gaps were preferred in both configurations, and the tested membranes showcased excellent salt rejection capabilities. These findings provide valuable insights into the potential applications of AGMD and VMD in desalination, especially in regions with water scarcity or pollution.

1. Introduction

Membrane distillation (MD) is a thermally driven process that involves the transport of water vapor across a hydrophobic membrane [1]. It is a relatively new process for the separation of liquids with low vapor pressures, such as water from aqueous solutions, and it can operate at temperatures much lower than those used in traditional distillation [2]. MD can use low-quality waste heat to create a vapor pressure difference across a hydrophobic membrane and create a high-quality distillate. The transmembrane driving force is the water vapor partial pressure gradient, which pushes the water vapor molecules across the membrane and collects them as a condensate on the permeate side [3]. The process is attractive because of its simplicity, energy efficiency, and scalability [4–7]. MD has been studied extensively in recent years due to its potential applications in water desalination, wastewater treatment, and other separation processes. From various water and wastewater sources, MD demonstrates promising water recovery [8,9]. Although reverse osmosis is still the most widely used desalination method, there is a chance of developing other low-energy separation methods, particularly for high-salinity streams [10]. The most significant advantage of the MD process over conventional desalination methods is its lower energy consumption, which is due to the process requiring low-grade energy associated with evaporation at ambient pressure [11,12].

A simulation study by Baghbanzadeh et al. on zero thermal input membrane distillation (ZTIMD) showed that ZTIMD is more economically effective than existing seawater desalination technologies and can produce pure water at a significantly lower cost of \$0.28/m^3 with a specific energy consumption of 0.45 kWh/m^3 [13]. ZTIMD process requires no external thermal input, as the enthalpy of the surface seawater is used to generate the necessary thermal energy, and the bottom seawater serves as the heat sink. The use of low-grade waste heat from industrial and/or power plants makes the MD process more viable for different applications. The waste heat from steam ejectors blow down, boiler blow down, dump condenser, flue gas chambers, etc. can be used for the MD process [14,15]. A simplified schematic diagram of the MD process is shown in Fig. 1 [16].

Abbreviations: AGMD, Air gap membrane distillation; AGS, Arabian gulf seawater; AR, Analytical reagent; DCMD, Direct contact membrane distillation; DI, Deionized water; DRP, Desalination research plant; KISR, Kuwait Institute for Scientific Research; LEP, Liquid entry pressure; MD, Membrane distillation; NaCl, Sodium chloride; PP, Polypropylene; PTFE, Polytetrafluro ethylene; PVDF, Polyvinylidene fluoride; SR, Salt rejection; SGMD, Sweeping gas membrane distillation; SWRO, Seawater reverse osmosis; TDS, Total dissolved solids; VMD, Vacuum membrane distillation; ZTIMD, Zero thermal input membrane distillation

* Corresponding author.
E-mail address: dr.hussain.alsairfi@gmail.com (H. Al-Sairfi).

https://doi.org/10.1016/j.dwt.2024.100145
Received 15 January 2024; Received in revised form 15 January 2024; Accepted 31 January 2024

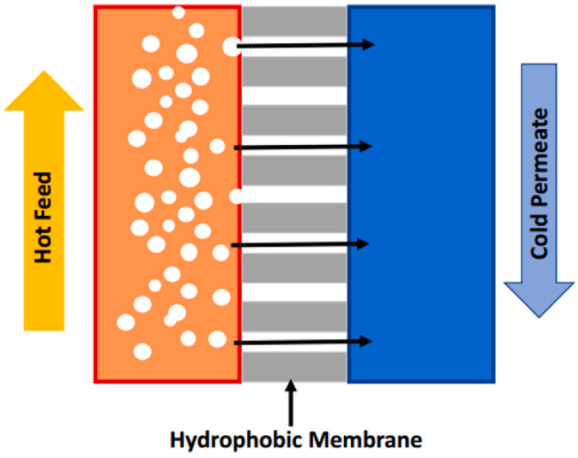

Fig. 1. The simplified flow diagram of the MD process [16, License number 5654670026479].

Other reported advantages of the MD process include high rejection rates for nonvolatile components [17,18]. It is feasible to operate with high solute concentrations in the feed or near-saturated solutions [19,20]. Additionally, the process is more compact and has a smaller footprint than traditional thermal distillation processes [18,21–23]. The MD process also operates at lower pressures than conventional pressure-driven membrane separation processes. This allows for flexibility in using less expensive piping materials and membranes with average mechanical properties [18,24,25]. Moreover, it does not require pretreatment chemicals [19]. Furthermore, MD operates at lower temperatures than conventional distillation [26], and it results in reduced vapor spaces compared to conventional distillation processes [26].

The most significant challenge of MD is the wetting of membranes in MD systems [27]. The wetting of membranes reduces permeate quality and can cause membrane fouling. Another major drawback is that the significant loss of energy supplied by the hot feed is lost by conduction through the membrane. As a result, a thermal boundary layer develops at the membrane surface due to the temperature differences between the membrane surface and the bulk solutions. This temperature polarization feature reduces the effectiveness of mass transportation [28].

There are four typical MD configurations, and they differ from each other in their approaches to collecting or condensing water. The four MD configurations are direct contact membrane distillation (DCMD), air gap membrane distillation (AGMD), sweeping gas membrane distillation (SGMD), and vacuum membrane distillation (VMD). Fig. 2 illustrates the four commonly used configurations of MD [29].

In DCMD, the condensing fluid temperature (i.e., pure water on the permeate side) is lower than in the feed-side liquid temperature. In this configuration, the hydrophobic microporous membrane is in direct touch with the liquid on both sides of the membrane [30]. The permeate from the feed side is collected by the pure water stream. Despite this being the most frequently employed in the lab-scale MD investigations, DCMD has not been widely used in pilot-scale MD systems because of its low energy efficiency and substantial conductivity losses caused by the membrane's interaction with both streams [31,32]. As a result, the integration of DCMD systems with other processes has been recommended by some research studies [33].

In AGMD, the vapor produced by the feed passes through the porous membrane and air gap and condenses on a coolant plate, which is cooled by the circulated cooling medium on the other side as shown in Fig. 2(b). Since the feed solution only comes into contact with the hot side of the membrane surface, and an additional air gap is introduced between the membrane and the condensation surface, less heat is lost through conduction, and the thermal efficiency of the AGMD system is higher than that of the DCMD system [28,34]. As a result, significantly larger temperature differences across the membrane are possible.

In SGMD, inert gas is used to sweep vapor on the permeate membrane side of the membrane module, allowing it to condense outside the membrane module. There is a gas barrier, as in AGMD, but an inert gas is blown over the permeate side of the membrane to reduce permeate-side mass-transfer resistance across the stagnant air-vapor film [35]. This increases the mass-transfer coefficient and can be used to remove volatile compounds from aqueous solutions. The permeate flux in SGMD, on the other hand, is affected by sweep gas velocity and air temperature at the module inlet [36].

In VMD, a vacuum pressure of 5–10 kPa is applied to the permeate side of the membrane to extract vapor. The vacuum reduces mass-transfer resistance and heat loss across the membrane. The vacuum on the permeate side raises the vapor pressure gradient across the membrane, increasing flux. An external condenser recovers vapor outside the module, as in SGMD [37,38]. Although increasing the vacuum pressure would result in higher permeate flux, exceeding the membrane's liquid entry pressure (LEP) could result in membrane wetting and performance degradation [39].

MD process performance is notably impacted by operating conditions and membrane properties. Significant factors include feed and coolant temperatures, concentrations, flow rates, permeate temperature, temperature differentials, mean temperature, permeate velocity, and vapor pressure difference [19,40,41].

In all MD configurations, higher feed temperatures lead to an exponential increase in permeate flux [19]. Keeping the feed input temperature constant and raising the coolant temperature reduces transmembrane vapor pressure, decreasing permeate flux [19,34]. Similarly, if the coolant temperature is fixed and feed temperature rises, transmembrane vapor pressure increases, resulting in higher permeate flux [40,41]. The Antoine equation explains this, as temperature influences vapor pressure due to its direct relation with diffusivity [34,42]. Elevated temperature enhances the mass-transfer coefficient and reduces temperature polarization as well [2].

Studies [1,2] reveal an inverse relationship between coolant side temperature and distillate flux. Lower temperatures yield higher distillate fluxes due to increased vapor pressure difference. The optimal flux occurs at the extremes of feed and permeate temperatures [1]. Feed concentration also affects permeate flux. Higher concentrations lead to lower vapor pressure, reducing flux. Additionally, as the surface membrane temperature declines with an increase in feed concentration, the heat transfer coefficient of the boundary layer also decreases [19,40]. Non-volatile compounds like sodium chloride decrease water activity. Elevated feed concentration enhances concentration polarization, decreasing the mass-transfer coefficient and heat-transfer coefficient on the feed side. Consequently, non-volatile solutions result in reduced permeate flux [31,40,43]. In the case of feed solutions with volatile components like alcohols, the impact of increasing feed concentration on permeate flux depends on the thermodynamic properties of the volatile compound and its interaction with water [40]. Higher volatile component concentration can elevate permeate flux due to increased vapor pressure.

Another factor influencing MD flux is the feed and cold side flow rates. Raising the feed flow rate enhances the heat transfer coefficient on the feed side, mitigating temperature and concentration polarization effects. Consequently, higher feed flow rates lead to increased distillate fluxes [34,40,41]. Studies indicate that a counter-current flow arrangement might offer superior heat and mass transfer efficiency compared to a co-current flow system [1]. In DCMD and SGMD systems, higher permeate flow rates enhance permeate-side heat transfer, reducing heat and concentration polarization. The elevated heat transfer coefficient on the permeate side aligns surface temperature with bulk permeate temperature, boosting driving force and permeate flow [19,40]. Conversely, in AGMD, the impact of the permeate-side flow rate on flux is negligible due to the dominant influence of the air gap [34,44]. Non-condensable gases in the feed can evolve with vapor upon heating, potentially obstructing membrane pores and causing mass-

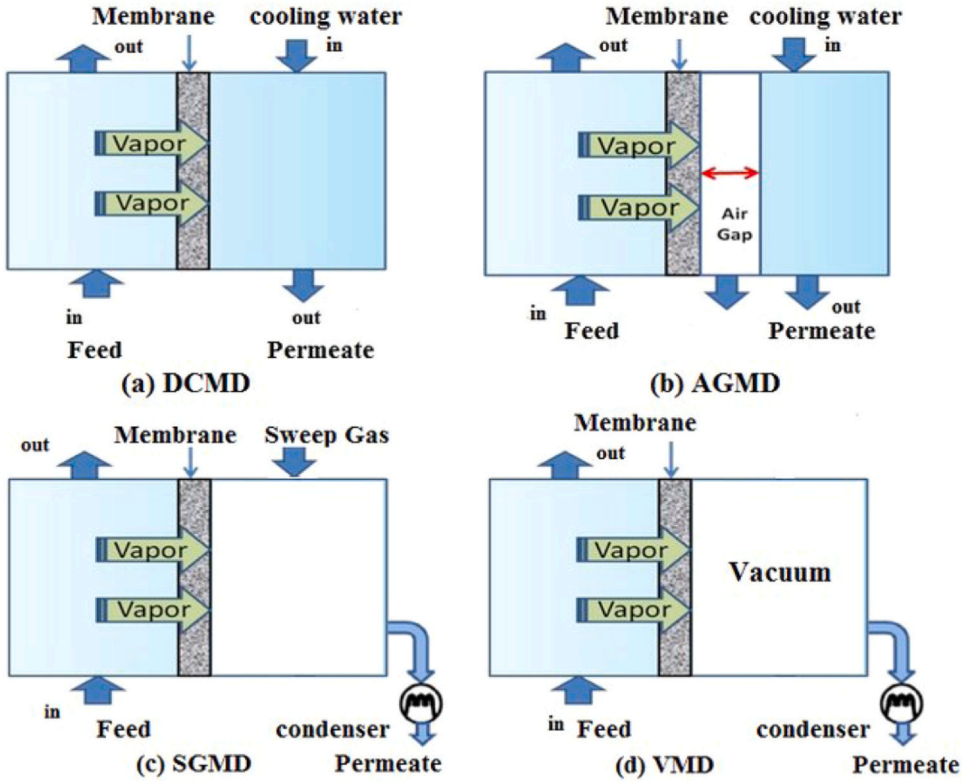

Fig. 2. Schematic representation of MD configurations [29].

transfer resistance, leading to reduced flux [45]. Removing these gases from feed and cold side solutions reduces partial pressure difference and enhances molecular diffusion through pores [45,46].

This paper presents a parametric study conducted at the Kuwait Institute for Scientific Research (KISR) to assess the feasibility of using AGMD and VMD processes for desalinating Arabian Gulf seawater (AGS) and oil field-produced water under various operating conditions. The current study is initially to present the laboratory-scale results of using AGMD and VMD technologies to treat AGS and oil field-produced water in Kuwait. This study is unique in terms of assessing the MD technology to desalinate the Arabian Gulf Seawater (AGS) which has stringent seawater chemistry compared to the other parts of the world. Also, the scope of the study is extended to treat the highly saline oil field-produced water samples (TDS ~ 168,000 ppm) collected from the state of Kuwait using the emerging AGMD and VMD configurations of the MD operation. The work is envisaged that the results of this laboratory-scale study in Kuwait can serve as a foundation for future pilot-scale studies utilizing AGMD and VMD technologies globally. Thus, this parametric study is a useful technique for evaluating the performance of the AGMD and VMD systems. Membrane distillation materials used should be hydrophobic and made from polymers to allow only vapour to pass through it. Thus, the current study was performed to assess the feasibility of using different commercial MD membranes towards desalination applications. The study utilized PP, PVDF, and PTFE membranes and, for the first time, investigated the effects of air gap depths and vacuum space in AGMD and VMD modules developed at KISR. AGMD and VMD are important to explore since they offer promising opportunities for desalination and water purification. They utilize temperature differences to generate water vapor, which is subsequently condensed to obtain purified water. AGMD and VMD processes have several advantages, including scalability, potential for integration with renewable energy sources, and high salt rejection capabilities. By studying these processes, we can gain insights into their performance, optimize their efficiency, and enhance their viability as potential solutions for addressing water scarcity and contamination issues worldwide. Additionally, exploring AGMD and VMD can contribute to the development of sustainable and efficient desalination technologies. The experimentation conducted is summarized in Table 1. This study is the first to report on the use of different vacuum spaces in a VMD process and to provide valuable insights into the treatment of different saline solutions using AGMD and VMD technology. The current study evaluated the viability of AGMD and VMD for treating different types of saline water, including Arabian Gulf seawater (AGS) and oil field-produced water. GCC countries mainly rely on seawater desalination technologies to fulfil the need for freshwater demand. Therefore research and development in exploring the advanced MD technology is requisite to address the issues of high energy and cost demand by the established desalination technologies. The treatment and management of high saline Oil field-produced water are the long term challenges faced by the oil-producing countries. Therefore, the current study further explores the treatment of oil field-produced water using MD technology.

2. Materials and methods

2.1. Experimental setup and procedure

Fig. 3 shows a photo of the bench-scale MD unit. The test unit can accommodate different MD configuration cells for testing. In this study, the flat sheet membranes with effective areas of 0.0155 m^2 and 0.003847 m^2 were used. The membrane modules, depicted in Figs. 4 and 5, were designed and built at KISR using Teflon and acrylic materials. The effect of channel depth was experimentally carried out on a 0.0155 m^2 membrane module. Currently, there are no commercially accessible membrane modules that offer the capability to adjust the depth of their channels. As a result, a new membrane module was designed and developed at the KISR to accommodate different plates 1 mm thick on the hot- and cold-channel sides. Figs. 4 and 5 show schematic representations and images of the VMD and AGMD cells, respectively. Figs. 6 and 7 show schematic representations of AGMD and VMD processes, respectively [47,48].

Table 1
Experimental framework and methodology.

Parameter		Reasoning
Feed Temperature,°C	65 to 85	The study investigated how AGMD and VMD systems respond to different feed solution temperatures, with a temperature range of 65–85 degrees Celsius commonly used in MD research. The maximum temperature tested was 85 °C to avoid thermal degradation of the membranes, which can occur at higher temperatures.
Flow rate, L/min	1.3-2.0	The experiment aimed to study the impact of varying feed flow rates on the performance of AGMD and VMD processes by measuring the resulting permeate flux. The goal was to establish data that provided insights into how the feed flow rate affects the performance of the two processes.
Feed solution concentration, wt %	NaCl solutions of 3.5–26%, oil field-produced water, Arabian Gulf seawater	To investigate the impact of varying feed concentrations on the permeate flux and to assess the viability of employing MD for feeds with varying levels of salt concentration including oil field-produced water and actual seawater
Membranes	Polypropylene, polyvinylidene fluoride and polytetrafluroethylene	To test the performance of different polymeric membranes for AGS desalination in the AGMD and VMD configurations

Flat sheet PP, PVDF, and PTFE membranes were used in this study. Merck Millipore Ltd. supplied the PVDF (YMJXSP3001) membrane, and Celgard 2500 supplied the PP membrane. The PTFE (PTFE023005) membranes were procured from the Sterlitech Corporation. The NaCl was analytical reagent (AR) grade, with a purity of 99.9%. (Techno Pharmchem, Sodium chloride AR – 33127). As a feed solution, NaCl solutions with concentrations of 3.5%, 7.0%, 15%, and 26% were used. The NaCl solutions were created by dissolving a known amount of NaCl salt in a known amount of deionized water (DI) produced by Millipore's ZRQSVP3WW | Direct-Q3 UV Water Purification System. Furthermore, AGS collected from a beach well at the KISR's Desalination Research Plant (DRP) in Kuwait was used as feed. The effectiveness of AGMD and VMD was also investigated for oil field-produced water collected from Kuwait Oil Company, Kuwait. The physiochemical analysis of the AGS used in this study is summarized in Table 2. The physiochemical analysis was carried out using a DR 5000 Spectrophotometer (Hach, DR 5000) and an ion chromatography system (Dionex 5000).

The experimental tests were carried out using a flat sheet membrane in an AGMD module and a VMD module. In the AGMD process, the hot feed solution is in direct contact with the membrane surface. The feed saline water is heated to the required temperature using a circulating bath (Cole Parmer Polystat – Item # EW-12122–02) and is pumped to the AGMD module. The coolant water temperature and flow are controlled using the circulating bath (Cole Parmer Polystat – Item # EW-12122–02). The air gap width was determined by the thickness of the stainless steel plate installed between the membrane and the condensation plate. The coolant water is in contact with the condensation plate. The vapor from the feed passes through the membrane pores and air gap which then becomes condensed on the stainless steel condensation plate. The condensed water was then collected, and flux was determined by measuring the increase in weight of the condensate water collected over time.

Weighting balance (MS32000L/A03, Mettler Toledo) was used to measure weight change. Regarding experimentation using the VMD configuration, the feed solution in the feed tank was heated to the required test temperature. At the required constant flow rate, heated water was pumped to the membrane module and back to the feed tank. At the same time, the vacuum pump and condenser both ran with the required constant vacuum pressure. The treated water was collected in a permeate water tank, and the weight of the collected water was measured. The same circulating bath and weighing balance used in AGMD were also used for the VMD experimentation.

Each experiment ran for 90 min after the system stabilized. The experiments were conducted three times, and the average value was used for the analysis. The membrane-active surface was directed toward the warm feed solution in both the AGMD and VMD experiments. All of

Fig. 3. MD test unit.

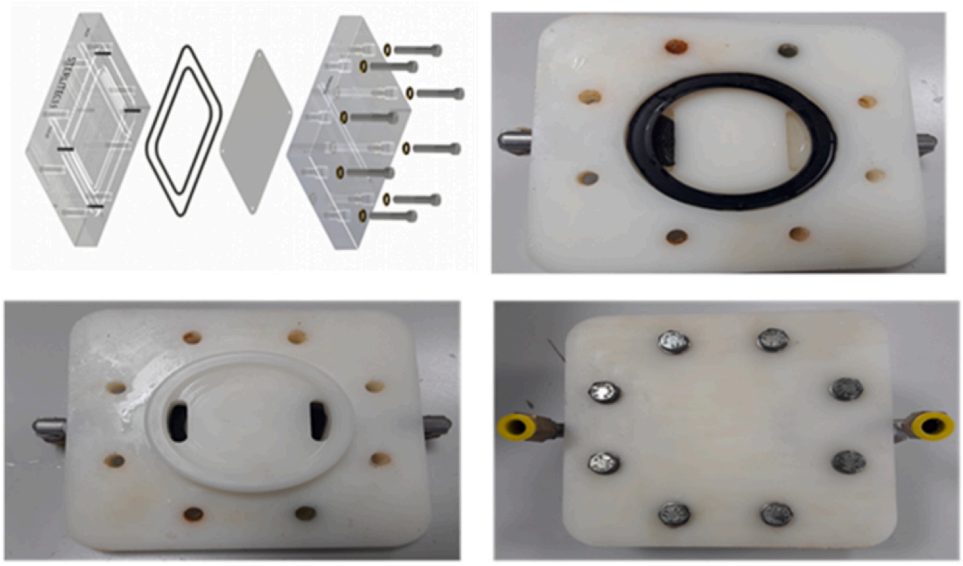

Fig. 4. Schematic representation and photos of the VMD cell.

the streams' temperatures and conductivities were also measured and recorded manually. Electrical conductivity, total dissolved solids (TDS), salinity, and temperature were manually measured using electrical conductivity meters (Thermo ScientificTM OrionTM Star A322 Conductivity Portable Meter).

The following equations were used to calculate the salt rejection efficiency (SR) and the water vapor flux:

$$SR = (1 - Cp/Cf)x100 \tag{1}$$

$$\text{WaterFlux} = \frac{\Delta\text{Weight}}{\text{Waterdensity} \times \text{membranesurfacearea} \times \Delta\text{time}} \tag{2}$$

where Cf and Cp are the concentrations of the feed and permeate, respectively.

The membranes used in the current work have been procured from the Sterlitech Corporation, USA and characterized. The main properties of the membrane used in the current study are porosity, pore size and thickness. The specifications and main characteristics of the applied various membranes in the current study are presented in Table 3.

3. Results and discussion

3.1. Influence of feed temperature

The effect of feed temperature on the permeate flux in the AGMD configuration is illustrated in Fig. 8 whereas Fig. 9 shows the influence of feed temperature on vapor flux in the VMD configuration. The examined temperature varied from 70 °C to 85 °C in the AGMD experimentation. The temperature on the cold side was maintained at 5 °C. The feed used was a 7% NaCl solution. Both the flow rate of the feed and the flow rate of the coolant solution were maintained at 1.3 L/min. To keep the condensing plate at the required temperature, deionized water was circulated on the cold side.

In the VMD experimentation, the feed temperatures were 65 °C, 75 °C, 80 °C, and 85 °C. The feed used was 7% NaCl solution. The vacuum pressure was kept at 100 kPa. The feed flow rate was 1.3 L/min. Although AGMD and VMD processes have similar principles, the presence or absence of a vacuum and the resulting pressure difference play a significant role in determining water flux. In AGMD, the water temperature is typically higher, as it is driven by a hot feed solution. The higher temperature promotes higher vapor pressure and greater vapor flow across the membrane, resulting in increased water flux. In the

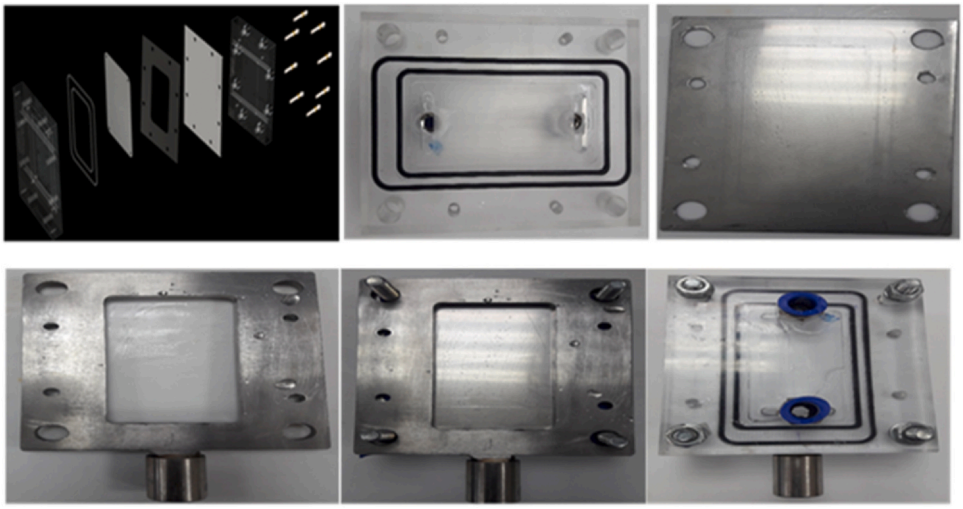

Fig. 5. Schematic representation and photos of the AGMD cell.

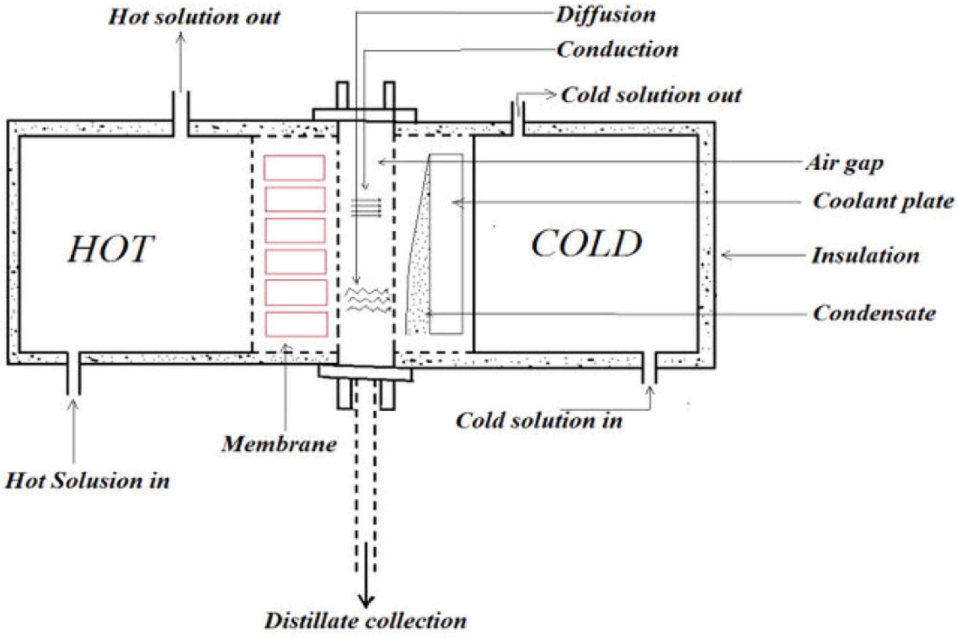

Fig. 6. Schematic representation of the AGMD process [47].

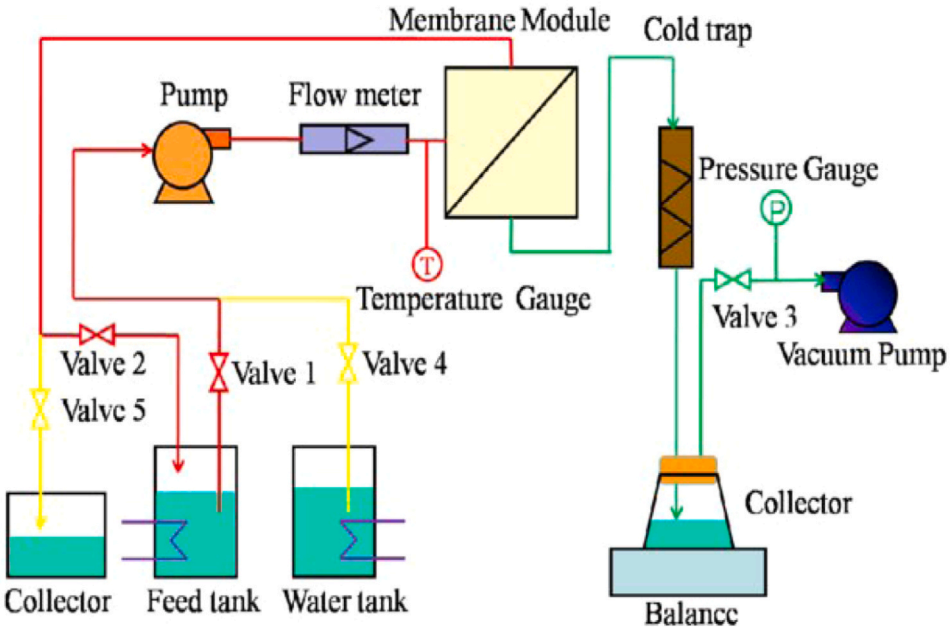

Fig. 7. Schematic representation of the VMD process [48].

Table 2
Physiochemical analysis of AGS.

Parameter	The average value in mg/L
TDS	43,415
Ca^{2+}	798.5
Mg^{2+}	1510.5
Na^{+}	13,397
$(SO_4)^{2-}$	3257
$(HCO_3)^{-}$	138.7
Cl^{-}	24,101
K^{+}	297
NO^{3-}	3.57

AGMD experimentation, when the temperature was increased from 70 °C to 85 °C, the permeate flux surged from 14.3 to 22.4 L/m^2h (i.e., an increase of 56.64%). On the other hand, in VMD, increasing the temperature from 65 °C to 85 °C at fixed vacuum value resulted in an increase in the permeate flux from 13.4 to 17.0 L/m^2h. The increase in flux with the increase in temperature was lower for the VMD configuration compared to the AGMD configuration. Therefore, using a vacuum as a driving force in the VMD configuration can increase the flux instead of relying on increased temperature.

The Antoine equation, which demonstrates that the effect of temperature on vapor pressure is relatively insignificant at low feed temperatures but becomes significant at higher feed temperatures, is the

Table 3
The main characteristics of the flat sheet membrane used in the current study.

Membrane	Code	Manufacturer	Pore size (μm)	Membrane thickness (μm)	Porosity %
Flat sheet (PP)	PP029025	Celgard 2500	0.064	25	55
Flat sheet (PTFE)	PTFE023005	Sterlitech	0.2	76 - 150	60 - 80
Flat sheet (PVDF)	YMJXSP3001	Merck Millipore Ltd.	0.3	150	60

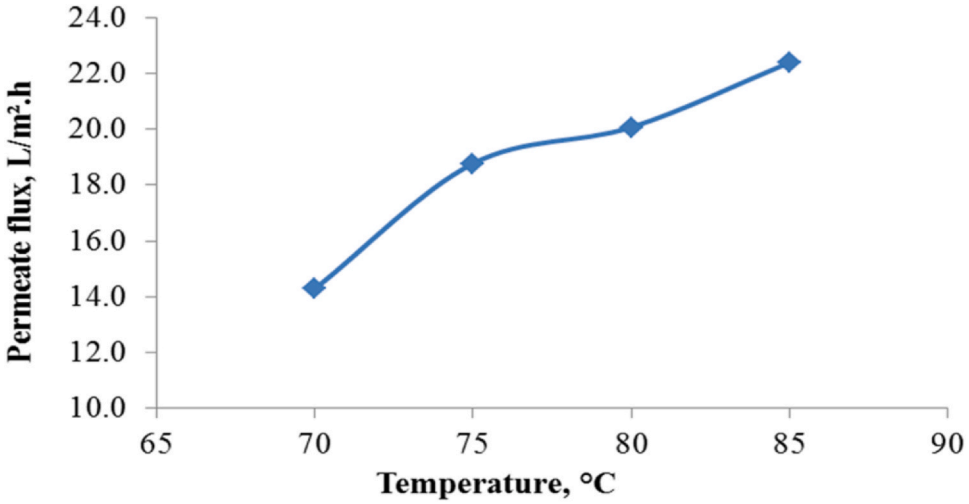

Fig. 8. Effect of feed temperature on the permeate flux in the AGMD configuration.

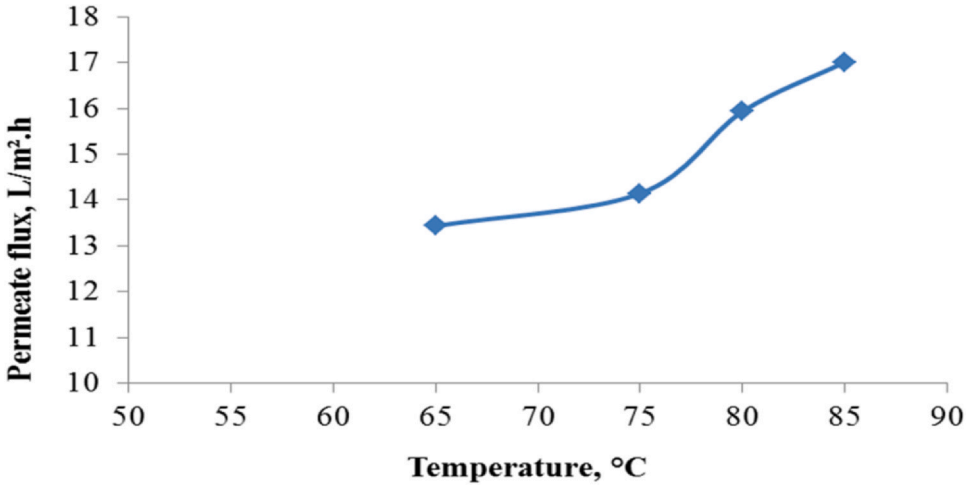

Fig. 9. Effect of feed temperature on the permeate flux in the VMD configuration.

one that best explains the reason for this process [49]. A small increase in temperature can lead to a significant rise in vapor pressure, and as a result, increasing the system's flux in proportion to that rise in vapor pressure. The findings of this study are in line with the studies reported in the literature [50,51]. When the temperature difference between the two sides of the membrane is raised, the diffusion coefficient is positively affected, resulting in increasing the vapor flux [50,51]. Also, the temperature polarization decreases as the feed temperature increases [52,53]. Since there is a direct correlation between temperature and diffusivity, the mass-transfer coefficient improves when working at higher temperatures [54].

Fig. 10 shows a comparison of permeate flux at different feed temperatures in AGMD and VMD configurations. It was observed that the permeate flux of AGMD increased more rapidly with temperature than that of VMD, which could be due to the enhanced driving force resulting from the temperature difference between feed and coolant streams in AGMD. It was observed that feed temperature has less effect on the salt rejection percentage by AGMD and VMD configurations. This demonstrates that both AGMD and VMD configurations using PP membranes can use high-temperature feeds to achieve high water flux while maintaining a good salt rejection percentage. In both configurations, the percentage of salt rejected was greater than 99.95%.

3.2. *Influence of solute concentration on feed*

Fig. 11 illustrates the impact of feed concentration on the permeate flux in an AGMD configuration. The feed used was a NaCl solution with concentrations of 3.5%, 7.0%, 15%, and 26%. AGS obtained from the DRP beach well was also utilized as feed. At the feed solution and coolant medium, the flow rate was 2 L/min. The utilized membrane was polypropylene. The temperatures on the feed side and the coolant side were 85 °C and 5 °C, respectively. On the coolant side of the AGMD module, deionized water was circulating. This study found that the permeate flux varied with feed concentration, with values of 26.35 L/

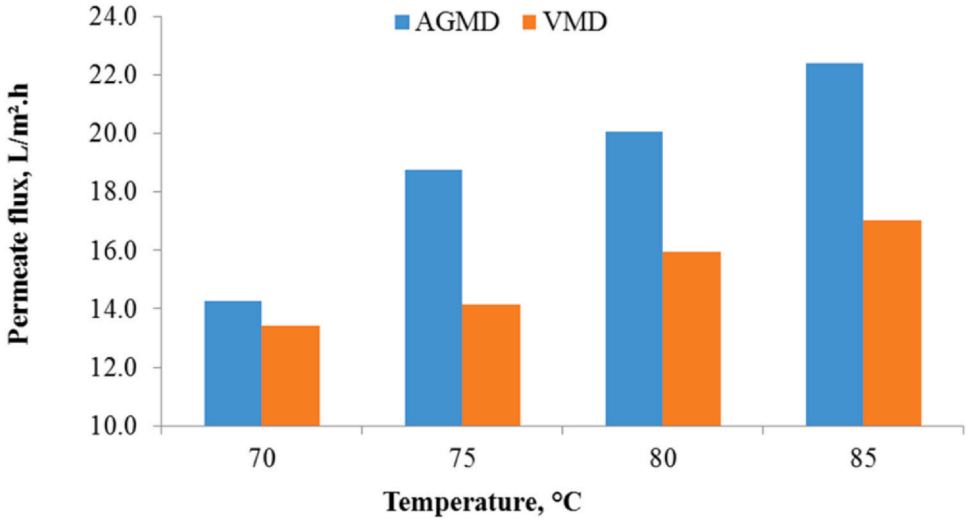

Fig. 10. Comparison of permeate flux at different feed temperatures in the AGMD and VMD configurations.

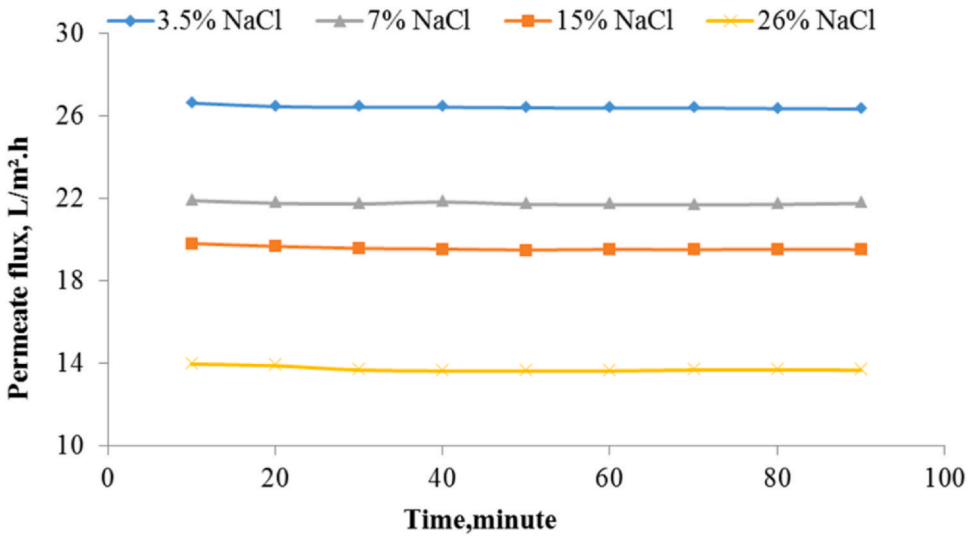

Fig. 11. Effect of feed concentration on permeate flux in the AGMD configuration.

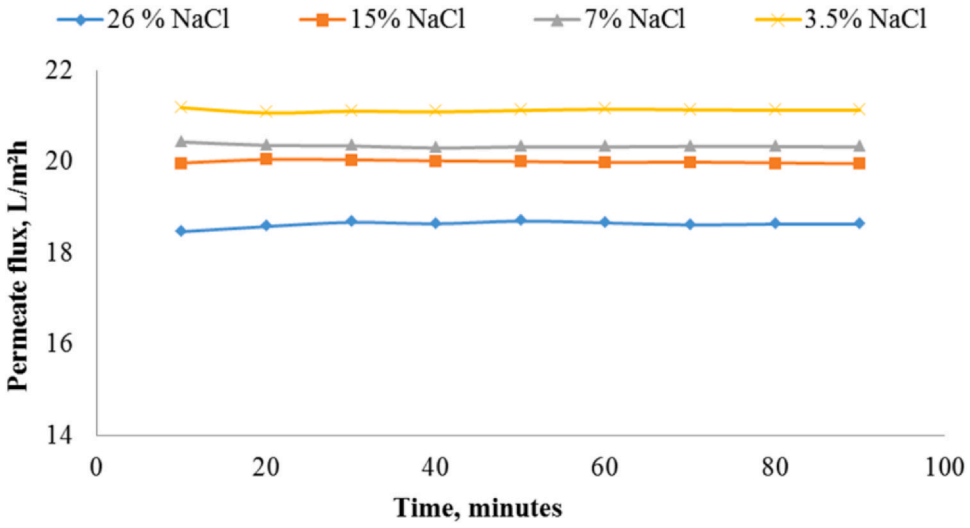

Fig. 12. Effect of feed concentration on permeate flux in the VMD configuration.

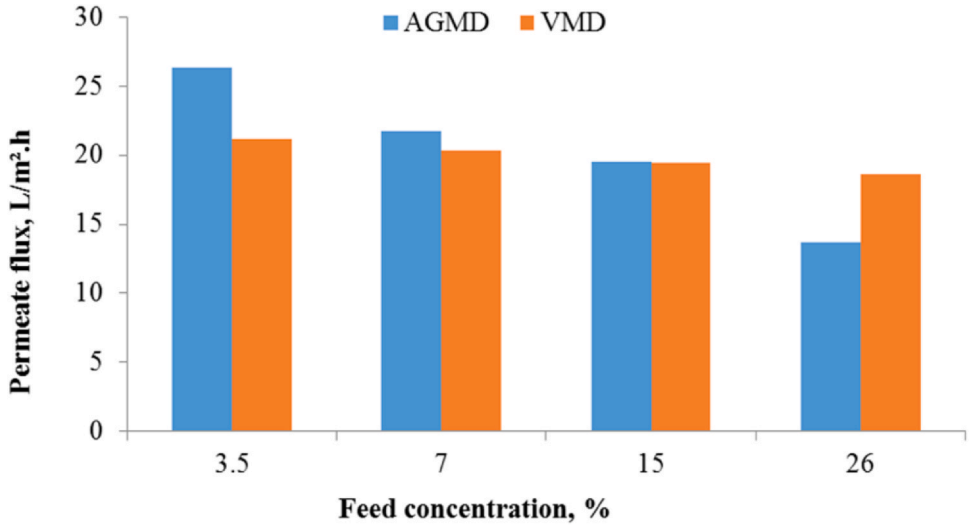

Fig. 13. Comparison of permeate flux at different feed concentrations in the AGMD and VMD configurations.

m^2.h, 21.77 L/m^2.h, 19.53 L/m^2.h, and 13.69 L/m^2.h observed for feed concentrations of 3.5%, 7%, 15%, and 26% NaCl, respectively. Fig. 12 shows how feed concentration affects the permeate flux in a VMD configuration. The NaCl concentrations of 3.5%, 7.0%, 15%, and 26% were used in the feed. The flow rate of the feed solution was 2 L/min. A PP membrane was used in the experiment. The feed-side temperature was 85 °C. The vacuum pressure was maintained at 100 kPa. For the VMD configuration, this study observed that the permeate flux decreased with increasing feed concentration, with values of 21.14 L/m^2.h, 20.33 L/m^2.h, 19.41 L/m^2.h and 18.64 L/m^2.h obtained for feed concentrations of 3.5%, 7%, 15%, and 26% NaCl, respectively.

Fig. 13 shows a simple comparison of the permeate flux in the AGMD and VMD configurations at different feed concentrations. It shows that the flux decreased with increasing feed concentrations in both the AGMD and VMD configurations. This observation supports the findings reported in other publications. When the feed concentration was increased from 3.5% to 7%, 15%, or 26%, the percentage reduction in permeate flux in the AGMD configuration was 17%, 26%, and 48%, respectively. However, compared to the results of the AGMD configuration, the reduction in flux with an increase in feed concentration was slightly lower in the VMD configuration. When the feed concentration was increased to 7%, 15%, and 26% from 3.5%, the percentage reductions in permeate flux in the VMD configuration were 5%, 10%, and 15%, respectively. Fig. 13 shows that the AGMD outperformed VMD at lower feed concentrations, while VMD performed well at higher feed concentrations. At higher feed concentrations, there is a chance of fouling and pores will become blocked by solute molecules. Due to the application of vacuum, fouling and pore blocking might have reduced and resulted in higher flux at higher concentrations in VMD.

The decrease in the flux with increasing feed concentrations could be caused by a reduction in water vapor pressure and increasing temperature polarization [50,55,56]. Another possible explanation for the decrease in the flux is a decline in water activity as the concentration increases. Furthermore, the mass-transfer coefficient of the boundary layer at the feed side decreases due to high-concentration polarization. Moreover, as the surface membrane temperature drops, the heat transfer coefficient at the boundary layer so does. All of these factors reduce the vapor pressure, which, in turn, reduces flux [57]. However, in contrast to other membrane desalination technologies, such as reverse osmosis, where high feed salinity negatively impacts system performance, the effect of feed concentration on permeate flux in all MD configurations is less significant.

The salt rejection percentage by AGMD and VMD configurations was found to be less affected by feed concentration. This showed that both AGMD and VMD configurations are appropriate for applications with relatively high feed concentrations. The amount of salt rejected in both configurations exceeded 99.5%.

3.3. *Influence of the recirculation flow rate*

The study examines the influence of recirculation rate on both sides of feed and coolant and uses the same flow for both sides when we increase or decrease the flow rate each time. The influence of the feed recirculation flow rate on permeate flux is shown in Fig. 14 under conditions of constant feed temperature and constant coolant temperature using a polypropylene membrane. The impact of feed flow on the AGMD configuration is depicted in Fig. 14, while Fig. 15 illustrates the effect of feed flow on the VMD setup. The tests were conducted using a 7% NaCl solution as the feed. The temperatures of the feed and coolant sides were 85 °C and 5 °C, respectively. The recirculation rate varied from 1.3 to 2.0 liters per minute. In the VMD configuration, the vacuum pressure was kept constant at 100 kPa. As presented in Figs. 14 and 15, an increase in water flux was observed as the flow rate increased. This observation is consistent with the literature [40,54,55].

It is suggested that a higher flow velocity improves flux by reducing temperature and concentration polarization in feed and coolant channels through improved mixing [58,59]. Srisurichan et al. reported that operating with a high recirculation rate reduces boundary layer resistance and increases the heat transfer coefficient, leading to a higher flux [54]. According to Chen et al., increasing the volumetric flow rate leads to increasing the fluid velocity, which in turn results in an improvement in the convective heat transfer coefficient and a reduction in the temperature polarization effect. This reduction in the temperature polarization effect enhances the permeate flux [58].

For the specific conditions in this study, increasing the flow velocity from 1.3 liters per minute to 2.0 liters per minute (i.e., 1.5-fold increases) led to a 1.2-fold increase in flux in the AGMD and VMD configurations. In the AGMD configuration, a rise of 18.1% (i.e., from 22.39 L/min.to 26.45 L/min) in the permeate flux was seen when the feed flow rate increased from 1.3 to 2.0 liters per minute, whereas the permeate flux increase rate was 19.9% (i.e., from 17.02 L/min.to 20.41 L/min) in the VMD configuration. In both the AGMD and VMD configurations, the salt rejection percentage was close to 99.9% and was largely unaffected by the feed recirculation rate.

Fig. 16 shows a simple comparison of the permeate flux in the AGMD and VMD configurations at different recirculation rates. It was observed that AGMD outperformed VMD at all recirculation flow rates, and the rate of increase in permeate flux with flow rate was almost the

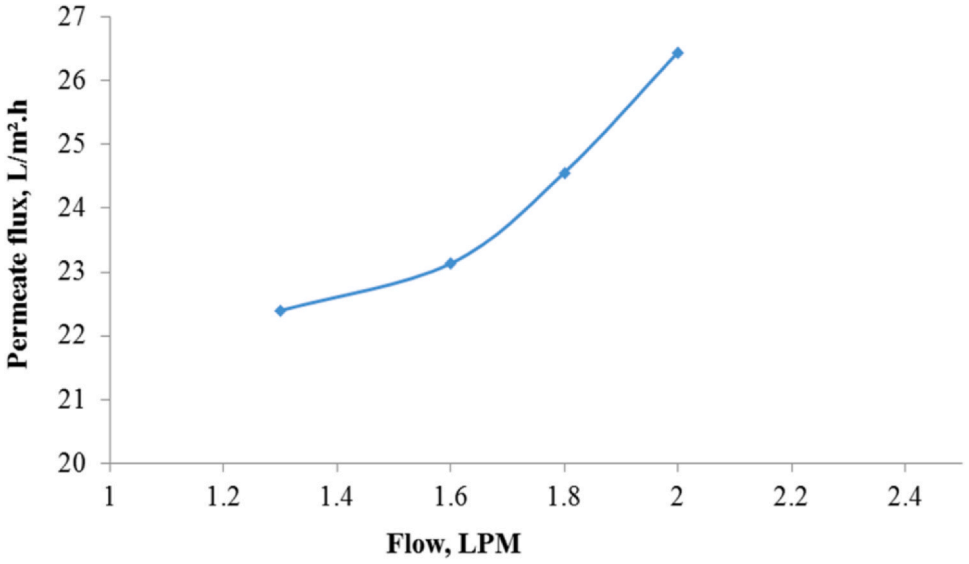

Fig. 14. Effect of recirculation flow rate on permeate flux in the AGMD configuration.

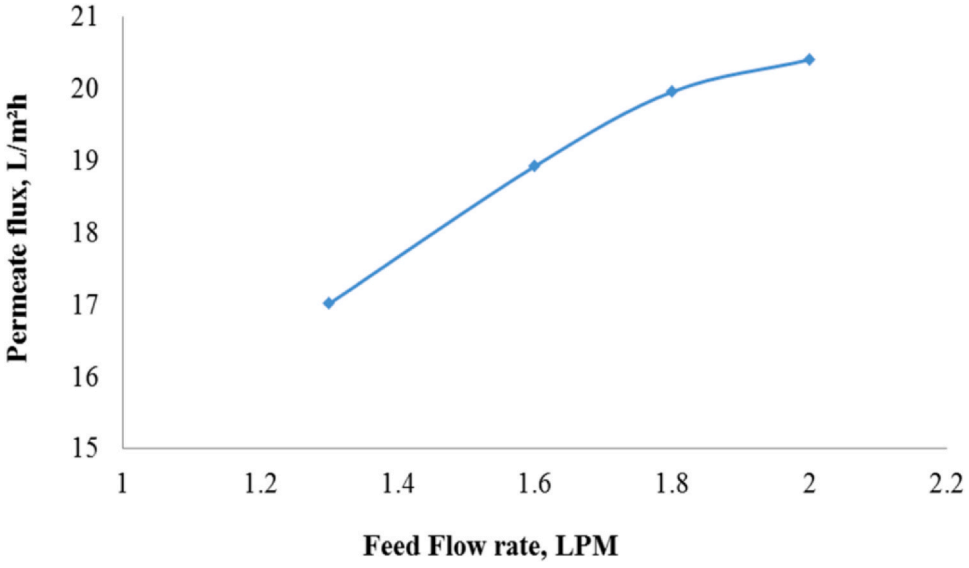

Fig. 15. Effect of recirculation flow rate on permeate flux in the VMD configuration.

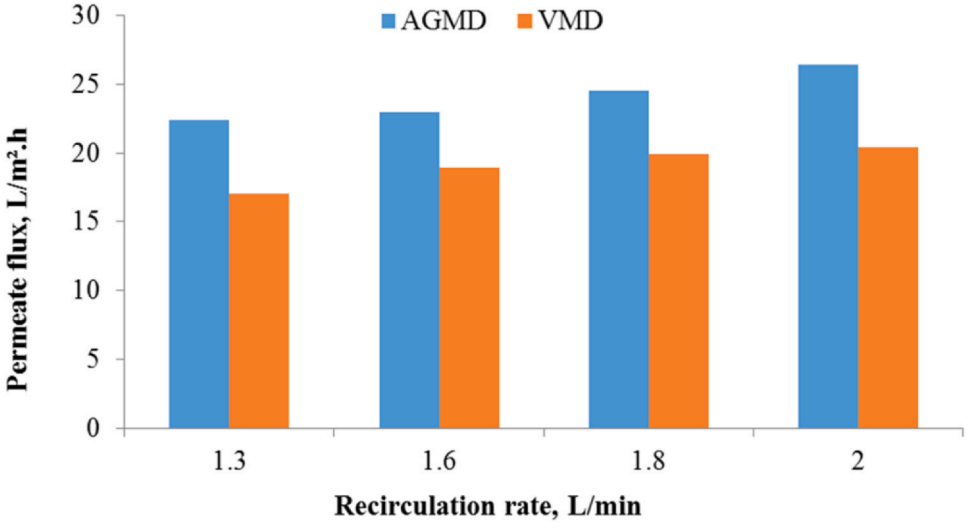

Fig. 16. Comparison of permeate flux in the AGMD and VMD configurations at different recirculation rates.

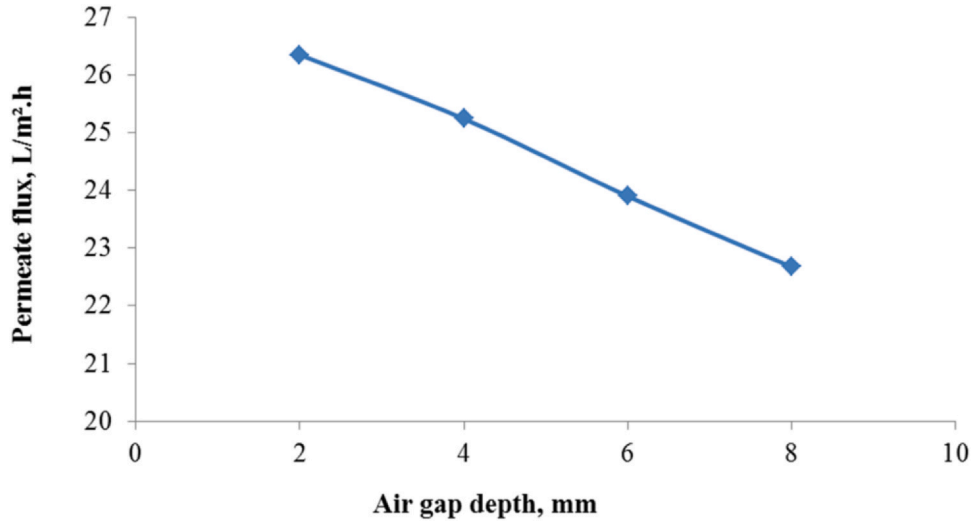

Fig. 17. The relationship between permeate flux and cold-channel depth in the AGMD configuration at a constant hot-channel depth.

same (i.e., a 1.2-fold increase) for the AGMD and VMD configurations. The permeate flux was not highly sensitive to an increase in the flow rate, and this may be because the main resistance of AGMD and VMD is located in the gap on the coolant side of the configurations, and there is less temperature polarization effect compared to other MD configurations, such as DCMD.

3.4. Influence of air gap depth and vacuum space on permeate flux

In the AGMD configuration, the initial set of experiments was carried out by varying the air gap depth (i.e., from 2 mm to 8 mm) while maintaining the hot-channel depth constant at 2 mm. Plates of 1 mm thickness were added to obtain the desired air gap between the membrane and the condensing plate. The next stage of AGMD experimentation includes experiments at a constant air gap (8 mm) and different feed-channel depths (2 mm to 8 mm). In the VMD configuration, in the initial phase of experimentation, the depth of the vacuum space varied from 2 mm to 8 mm by adjusting the number of plates added between the membrane and the cold trap while keeping the depth of the feed-channel constant at 2 mm. The vacuum space is the empty channel that comes after the membrane where the vapour comes on and is vacuumed through a vacuum pump to the condenser outside the vacuum space.

The next stage of the VMD experimentation was performed at a constant vacuum space depth (8 mm) but with varying depths of the feed channel from 1 mm to 8 mm. In both configurations, the membrane tested was a polypropylene membrane. The feed solution was a 7% NaCl solution at 85 °C, and the coolant used in the AGMD configuration was deionized water at 5 °C, both flowing at a rate of 2 L/min. Fig. 17 shows the relationship between permeate flux and cold-channel depth in the AGMD configuration. It was observed that the percentage of permeate flux decrease was 16% when the cold-channel depth was increased to 8 mm from 2 mm. Fig. 18 shows the relationship between the permeate flux and hot-channel depth in the AGMD configuration. It was observed that the percentage of permeate flux decrease was 34.6% when the hot-channel depth was increased to 8 mm from 1 mm. This observation is in line with the literature [46,57,59].

Banat and Simandl (1994), found that reducing the width of the gap leads to a rise in the temperature gradient and, as a result, an increase in the permeate flux [44]. Reducing channel depth may lead to a higher concentration of thermal energy within a smaller space. Accordingly, the temperature distribution will be almost uniform within the space. Upon increasing the gap width, there may be a nonuniform temperature distribution within the space. The temperature gradient between the feed channel and the cold channel might have been higher at lower channel depths, and this could have produced more flux.

Fig. 19 shows the relationship between permeate flux and vacuum space in the VMD configuration. It was observed that the percentage of the permeate flux increase was 28% when the vacuum space depth was

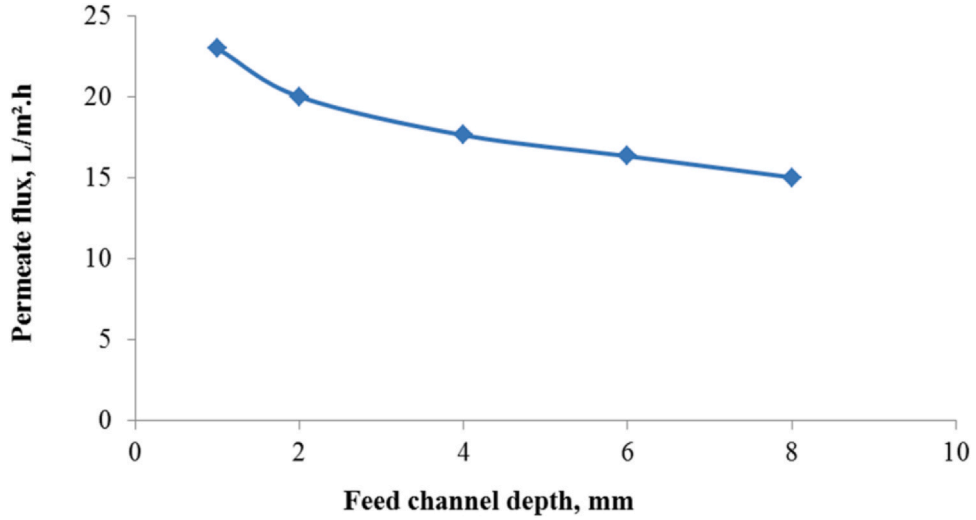

Fig. 18. The relationship between permeate flux and feed-channel depth in the AGMD configuration at a constant cold-channel depth.

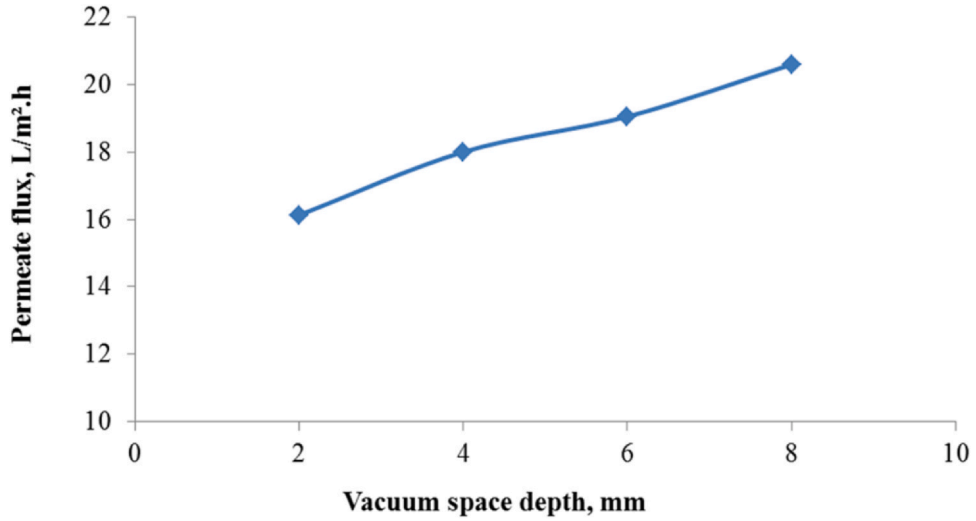

Fig. 19. The relationship between permeate flux and vacuum space depth in the VMD configuration at a constant hot-channel depth.

increased from 2 mm to 8 mm. Fig. 20 shows the relationship between permeate flux and hot-channel depth in the VMD configuration. It was observed that the percentage of the permeate flux increase was 15.5% when the hot-channel depth was increased from 2 mm to 8 mm. It can be observed that the AGMD and VMD systems' responses to channel depth variation studies were different.

In the AGMD configuration, permeate flux decreased with increasing the feed channel and air gap depths, whereas the increase in the permeate flux with feed channel and vacuum space depths was observed in the VMD experiments. Increasing the vacuum space led to an increase in permeate flux, with a non-linear relationship observed between the two. Specifically, when the vacuum space was increased four times, the resulting increase in flux was only 1.3 times. This nonlinear relationship could be due to several factors, including limitations in mass transfer or heat transfer across the membrane surface, saturation of the driving force for mass transfer, or potential changes in the properties of the membrane or feed solution at high vacuum levels.

The observed higher flux at low gaps in the AGMD shows that the lower gaps are preferred in AGMD configurations. However, since increasing the vacuum space has a significant effect on permeate flux, the higher gaps can be considered for the VMD configurations. The good flux at lower gaps in the AGMD could be attributed to the reduced effects of the heat and mass-transfer mechanisms at smaller gaps. At smaller gaps, there is less distance for heat and mass transfer to occur, leading to a potential decrease in temperature polarization and concentration polarization effects. This could result in higher flux rates. However, it is important to note that the specific mechanisms underlying this behavior may vary depending on the experimental setup and conditions, and further studies are needed to fully understand the observed behavior.

3.5. Performance of AGMD and VMD processes for treating Oil Field-Produced water and AGS

We investigated the feasibility of using the AGMD and VMD systems to treat oil field-produced water using water directly as feed without any pretreatment. In the AGMD process, deionized water was used as the cooling medium, with a feed temperature of 85 °C. The VMD experimentation was carried out at feed temperatures of 80 °C and 85 °C. The cooling side temperature was 5 °C for both AGMD and VMD processes. The feed and cooling solution channels were operated at a flow rate of 2 L/min. The AGMD experimentation was carried out with an air gap depth of 8 mm, while the VMD experimentation was conducted with a vacuum space of 8 mm. The experiment was conducted using a polypropylene membrane. The permeate flux obtained was 15 L/m^2.h in the AGMD experimentation at 85°C.

Fig. 21 shows the permeate flux obtained from the VMD experimentation using oil field-produced water as feed at 80 °C and 85 °C. It

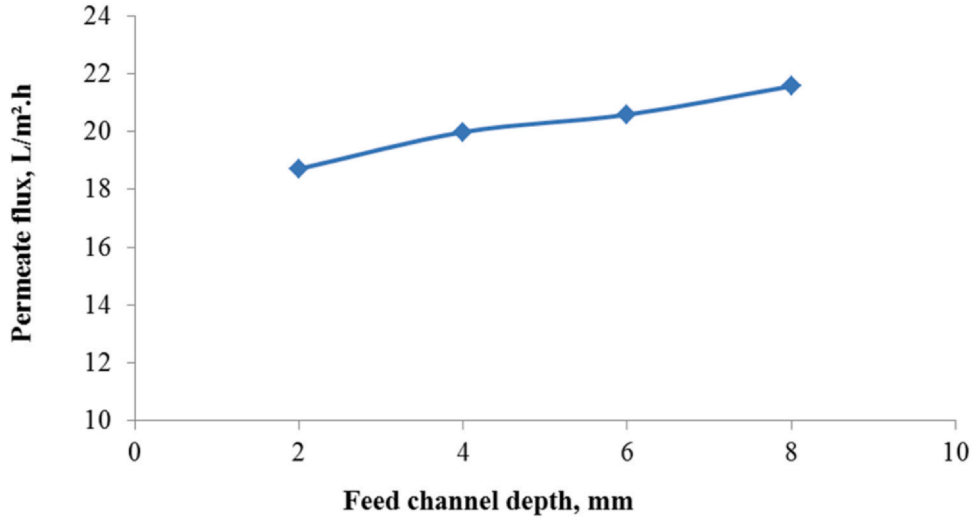

Fig. 20. The relationship between permeate flux and hot-channel depth in the VMD configuration in a constant vacuum space.

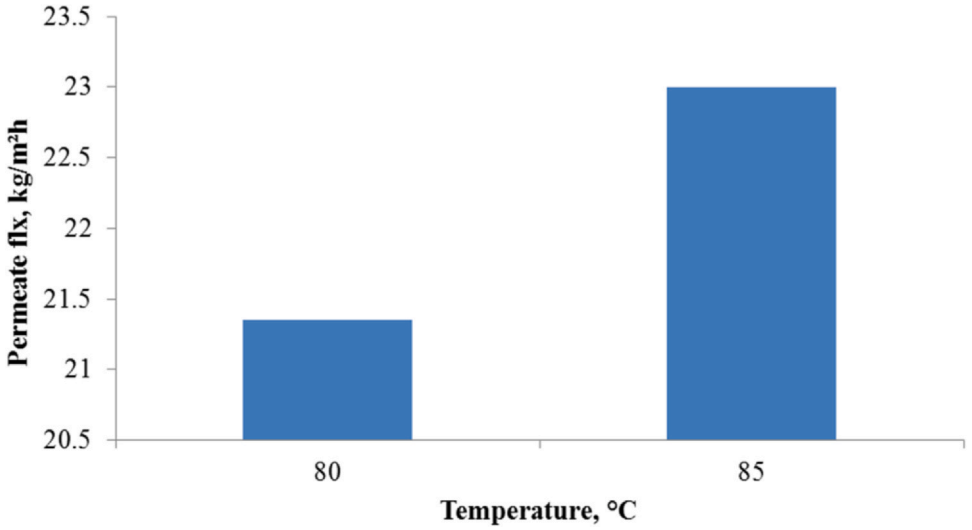

Fig. 21. Permeate flux obtained from the VMD experimentation using oil field-produced water as feed at 80 °C and 85 °C.

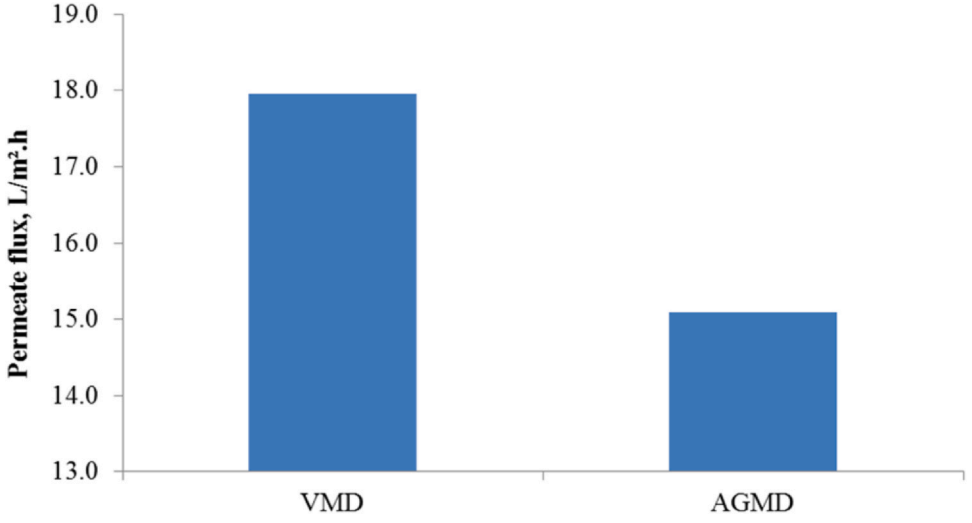

Fig. 22. Permeate flux obtained from VMD and AGMD experimentation using AGS obtained from beach well as feed at 85 °C.

Table 4
Chemical analysis results of oil field-produced water and permeate water obtained from AGMD and VMD processes.

Parameter	Unit	Feed water	AGMD Permeate water	VMD Permeate water
Total dissolved solid (TDS)	mg/L	168,000	17	364
Total suspended solid (TSS)	mg/L	95	< 2	2
Chloride	mg/L	99,420	12	214
Oil & Grease	mg/L	71.8	< 0.75	< 0.75
Total organic carbon (TOC)	mg/L	9.5	3.4	3.4
Turbidity	NTU	64	0.5	1.3

Table 5
Water flux and salt rejection percentages of the PP, PVDF, and PTFE membranes were tested under a VMD configuration at different temperatures using a 7% NaCl solution as the feed.

Membrane	Temperature, °C	Water Flux, L/m²h	Salt Rejection, %
PP	80	15.6	99.97
	85	17.8	99.98
PVDF	80	104.2	99.97
	85	112.1	99.97
PTFE	80	11.5	99.97
	85	13.3	99.97

was observed that there was a linear increase in the permeate flux with temperatures. The permeate flux was 23 L/m^2.h and 21.35 L/m^2.h at 85 °C and 80 °C, respectively. The experimental results show that both AGMD and VMD processes were highly efficient in treating oil field-produced water. Fig. 22 shows the permeate flux obtained from the AGMD and VMD experiments using AGS obtained from beach wells and feed at 85 °C.

Based on the experimental results shown in Fig. 22, the VMD exhibited a higher permeate flux of 18 L/m^{2}h compared to AGMD's permeate flux of 15.1 L/m^{2}h, indicating that the VMD is a more effective process for treating AGS obtained from a beach well at 85 °C. Therefore, these findings suggested that the VMD may be a preferable process for seawater desalination when compared to AGMD. Table 4

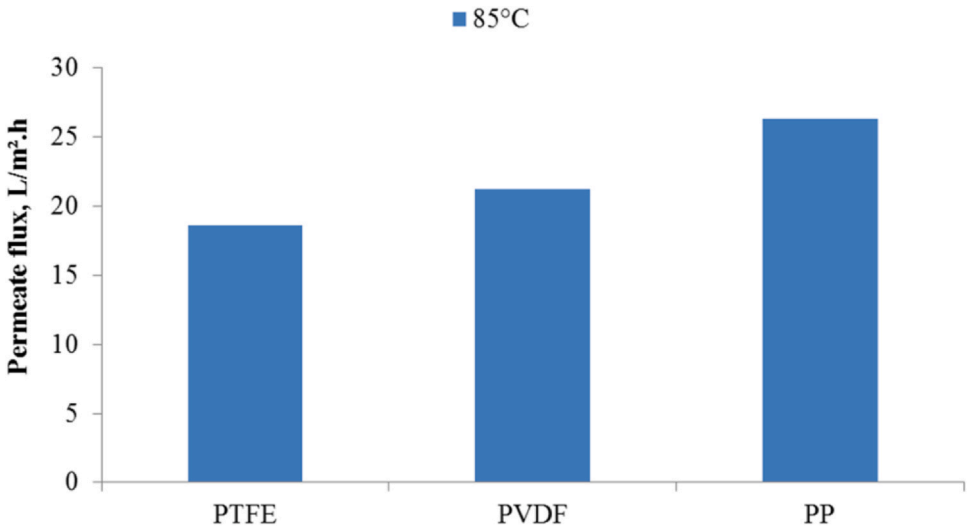

Fig. 23. Water flux of the PP, PVDF, and PTFE membranes tested under the AGMD configuration at 85 °C using a 7% NaCl solution as feed.

shows the analytical results of the feed water sample and permeate collected after the AGMD and VMD experiments. It can be observed that the VMD process performed slightly better than the AGMD process in treating oil field-produced water. The permeate TDS values show that salt rejection was almost 99.9% in both the AGMD and VMD processes. However, further studies are required to study the long-term performance of AGMD and VMD processes for treating oil field-produced water.

3.6. The performance of PP, PVDF, and PTFE membranes in the AGMD and VMD process

The effectiveness of flat sheet membranes made of PP, PVDF, and PTFE was examined in the AGMD and VMD processes using a 7% NaCl solution as the feed. The VMD tests were performed at feed temperatures of 80 °C and 85 °C, with a cooling side temperature of 5 °C. In the AGMD process, deionized water was utilized as the cooling medium, and the feed temperature was set at 85 °C. The water flux and salt rejection percentages of the PP, PVDF, and PTFE membranes are summarized in Table 5. The water flux increased with an increase in temperature for the PP, PVDF, and PTFE membranes. The order of fluxes observed in the VMD configuration is PVDF > PP > PTFE. The results showed that the tested membranes achieved salt rejections as high as 99.97%. PTFE membranes showed an increase of 16.1% in flux with an increase in temperature from 80 °C to 85 °C. The flux increased by 14.2% and 7.6% for the PP and PVDF membranes, respectively. Fig. 23 shows the performance behavior of the PP, PVDF, and PTFE membranes in the AGMD configuration. It was observed that the order of fluxes observed in the AGMD configuration is PP > PVDF > PTFE.

4. Conclusion

This study investigated the viability of air gap membrane distillation (AGMD) and vacuum membrane distillation (VMD) for desalinating different types of saline water. Experiments were conducted to evaluate the impact of factors such as feed temperature, feed concentration, recirculation flow rate, air gap, vacuum space depth, and membrane types (PP, PVDF, PTFE) on permeate flux in AGMD and VMD configurations. The results showed that increasing the feed temperature led to increased permeate flux in both configurations, but AGMD achieved a greater increase. The permeate flux decreased with increasing feed concentration, with AGMD showing a higher reduction than VMD. The recirculation flow rate had a positive impact on permeate flux in both configurations, and AGMD outperformed VMD consistently. The study also explored the influence of channel depths on permeate flux and found that AGMD and VMD responded differently. The experiments demonstrated high efficiency in treating oil field-produced water and AGS, with both configurations exhibiting excellent salt rejection capabilities. The permeate flux obtained was 15 L/m2.h in AGMD at 85 °C, and in VMD, the permeate flux linearly increased with a flux of 23 L/m2.h at 85 °C, indicating that VMD may be a preferable process for seawater desalination when compared to AGMD. Salt rejection was almost 99.9% in both AGMD and VMD, with VMD performing slightly better than AGMD in treating oil field-produced water. The study provides insights into the potential applications and optimization of AGMD and VMD processes for desalination purposes, emphasizing the need for further research at both laboratory and pilot scales.

Declaration of Competing Interest

The authors declare that they have no known competing financial interests or personal relationships that could have appeared to influence the work reported in this paper.

Acknowledgment

The authors would like to express their gratitude to the Water Research Centre of the KISR for providing us with the facilities necessary to conduct our experimental investigations as well as for their timely supervision to ensure that our work was completed efficiently.

References

[1] Manawi YM, Khraisheh M, Fard AK, Benyahia F, Adham S. Effect of operational parameters on distillate flux in direct contact membrane distillation (DCMD): comparison between experimental and model predicted performance. Desalination 2014;336:110–20.
[2] Adham S, Hussain A, Matar JM, Dores R, Janson A. Application of membrane distillation for desalting brines from thermal desalination plants. Desalination 2013;314:101–8.
[3] Kalla S, Piash KS, Sanyal O. Anti-fouling and anti-wetting membranes for membrane distillation. J Water Process Eng 2022;46:102634.
[4] Kabeel AE, Abdelgaied M, El-Said MS. Study of a solar-driven membrane distillation system: evaporative cooling effect on performance enhancement. Renew Energy 2017;106:192–200.
[5] Leblanc J, Akbarzadeh A, Andrews J, Lu H, Golding P. Heat extraction methods from salinity-gradient solar ponds and introduction of a novel system of heat extraction for improved efficiency. Sol Energy 2011;85(12):3103–42.
[6] Christie KS, Horseman T, Lin S. Energy efficiency of membrane distillation: simplified analysis, heat recovery, and the use of waste-heat. Environ Int 2020;138:105588.
[7] Singh D, Sirkar KK. Desalination of brine and produced water by direct contact membrane distillation at high temperatures and pressures. J Membr Sci 2012;389:380–8.

[8] Biniaz P, Torabi AN, Makarem MA, Rahimpour MR. Water and wastewater treatment systems by novel integrated membrane distillation (MD). Chem Eng 2019;3(1):8.
[9] Yan Z, Jiang Y, Liu L, Li Z, Chen X, Xia M, et al. Membrane distillation for wastewater treatment: a mini review. Water 2021;13:3480.
[10] Swaminathan J, Chung HW, Warsinger DM. Energy efficiency of membrane distillation up to high salinity: evaluating critical system size and optimal membrane thickness. Appl Energy 2018;211:715–34.
[11] Bahar R, Hawlader M, Ariff T. Channeled coolant plate: a new method to enhance freshwater production from an air gap membrane distillation (AGMD) desalination unit. Desalination 2015;359:71–81.
[12] C. Liu and A. Martin, Membrane Distillation and Applications for Water Purification in Thermal Cogeneration - A Prestudy, Technical Report, Report Number: VARMEFORSK-909, (2005) Vaermeforsk, Stockholm (Sweden).
[13] Baghbanzadeh M, Rana D, Lan CQ, Matsuura T. Zero thermal input membrane distillation, a zero-waste and sustainable solution for freshwater shortage. Appl Energy 2017;187:910–28.
[14] González D, Amigo J, Suárez F. Membrane distillation: perspectives for sustainable and improved desalination. Renew Sustain Energy Rev 2017;80:238–59.
[15] Adham S, Hussain A, Matar JM, Dores R, Janson A. Application of membrane distillation for desalting brines from thermal desalination plants. Desalination 2013;314:101–8.
[16] Ahmed FE, Lalia BS, Hashaikeh R, Hilal N. Alternative heating techniques in membrane distillation: a review. Desalination 2020;496.
[17] Chiam CK, Sarbatly R. Evolution of membrane surface properties for membrane distillation: a mini review. J Appl Membr Sci Technol 2022;26(3):45–64.
[18] Leaper S, Abdel-Karim A, Gad-Allah TA, Gorgojo P. Air-gap membrane distillation as a one-step process for textile wastewater treatment. Chem Eng J 2019;360:1330–40.
[19] Kiss AA, Readi OMK. An industrial perspective on membrane distillation processes. J Chem Technol Biotechnol 2018;93(8):2047–55.
[20] H. Susanto, Towards practical implementations of membrane distillation, chemical engineering and processing: process intensification, 50(2) (2011) 139–150.
[21] Deshmukh A, Boo C, Karanikola V, Lin S, Straub AP, Tong T, et al. Membrane distillation at the water-energy nexus: limits, opportunities, and challenges. Energy Environ Sci 2018;11(5):1177–96.
[22] Hickenbottom KL, Cath TY. Sustainable operation of membrane distillation for enhancement of mineral recovery from hypersaline solutions. J Membr Sci 2014;454:426–35.
[23] Duong HC, Chivas AR, Nelemans B, Duke M, Gray S, Cath TY, et al. Treatment of RO brine from CSG produced water by spiral-wound air gap membrane distillation—a pilot study. Desalination 2015;366:121–9.
[24] Wang P, Chung TS. Recent advances in membrane distillation processes: membrane development, configuration design and application exploring. J Membr Sci 2015;474:39–56.
[25] Bagci PO. Potential of membrane distillation for production of high quality fruit juice concentrate. Crit Rev Food Sci Nutr 2015;55(8):1098–113.
[26] Qtaishat MR, Banat F. Desalination by solar powered membrane distillation systems. Desalination 2013;308:186–97.
[27] Thomas N, Mavukkandy MO, Loutatidou S, Arafat HA. Membrane distillation research & implementation: lessons from the past five decades. Sep Purif Technol 2017;189:108–27.
[28] Alkhudhiri A, Darwish N, Hilal N. Membrane distillation: a comprehensive review. Desalination 2012;287:2–18.
[29] Alanezi AA, Safaei MR, Goodarzi M, Elhenawy Y. The effect of inclination angle and reynolds number on the performance of a direct contact membrane distillation (DCMD) process. Energies 2020;13(11):2824.
[30] Francis L, Ahmed FE, Hilal N. Advances in membrane distillation module configurations. Membranes 2022;12(1):81.
[31] Khayet M. Membranes and theoretical modeling of membrane distillation: a review. Adv Colloid Interface Sci 2011;164:56–88.
[32] Eykens L, Hitsov I, De Sitter K, Dotremont C, Pinoy L, Van B. der Bruggen, Direct contact and air gap membrane distillation: differences and similarities between lab and pilot scale. Desalination 2017;422:91–100.
[33] Ashoor BB, Mansour S, Giwa A, Dufour V, Hasan SW. Principles and applications of direct contact membrane distillation (DCMD): a comprehensive review. Desalination 2016;398:222–46.
[34] Alklaibi A, Lior N. Comparative study of direct-contact and air-gap membrane distillation processes. Ind Eng Chem Res 2007;46:584–90.
[35] Gude GG. Emerging technologies for sustainable desalination handbook (An imprint of Elsevier). Oxford OX5 1GB, United Kingdom: Butterworth-Heinemann Publications; 2018. p. 55–106. (An imprint of Elsevier).
[36] P. Pal, Groundwater Arsenic Remediation: Treatment Technology and Scale UP, Butterworth-Heinemann Publications, Oxford OX5 1GB, United Kingdom 2015, pp. 179–270.
[37] Rahimpour MR, Kazerooni NM, Parhoudeh M. Chapter 8—water treatment by renewable energy-driven membrane distillation. Current Trends and Future Developments on (Bio-) Membranes. Amsterdam: Elsevier; 2019. p. 179–211.
[38] Kim H, Yun T, Hong S, Lee S. Experimental and theoretical investigation of a high performance PTFE membrane for vacuum-membrane distillation. J Membr Sci 2021;617:118524.
[39] Alsaadi AS, Francis L, Amy GL, Ghaffour N. Experimental and theoretical analyses of temperature polarization effect in vacuum membrane distillation. J Membr Sci 2014;471:138–48.
[40] El-Bourawi MS, Ding Z, Ma R, Khayet M. A framework for better understanding membrane distillation separation process. J Membr Sci 2006;285:4–29.
[41] J. Walton, H. Lu, C. Turner, S. Solis and H. Hein, Final Report titled “Solar and waste heat desalination by membrane distillation”, Desalination Research and Development Program Agreement Number: 98-FC-81–0048, College of Engineering University of Texas at El Paso El Paso, Texas, 2000.
[42] Kullab A, Martin A. Membrane distillation and applications for water purification in thermal cogeneration plants. Sep Purif Technol 2011;76(3):231–7.
[43] Khayet M, Mengual J, Matsuura T. Porous hydrophobic/hydrophilic composite membranes: application in desalination using direct contact membrane distillation. J Membr Sci 2005;252:101–13.
[44] Banat F, Simandl J. Theoretical and experimental study in membrane distillation. Desalination 1994;95:39–52.
[45] Martínez L, Florido-Díaz FJ. Theoretical and experimental studies on desalination using membrane distillation. Desalination 2001;139:373–9.
[46] Alklaibi A, Lior N. Membrane-distillation desalination: status and potential. Desalination 2004;171:111–31.
[47] Bappy MJP, Bahar R, Ibrahim Sh, Ariff TF. Enhanced freshwater production using finned-late air gap membrane distillation (AGMD). MATEC Web Conf 2017;103:06014.
[48] Hu C, Yang Z, Sun Q, Ni Z, Yan G, Wang Z. Facile preparation of a superhydrophobic iPP microporous membrane with micron-submicron hierarchical structures for membrane distillation. Polymers 2020;12(4):962.
[49] Khayet M, Matsuura T. Membrane Distillation Principles and Applications. Amsterdam, The Netherlands: Elsevier; 2011.
[50] Qtaishat M, Matsuura T, Kruczek B, Khayet M. Heat and mass transfer analysis in direct contact membrane distillation. Desalination 2008;219(1–3):272–92.
[51] Gunko S, Verbych S, Bryk M, Hilal N. Concentration of apple juice using direct contact membrane distillation. Desalination 2006;190(1–3):117–24.
[52] Phattaranawik J, Jiraratananon R, Fane AG. Heat transport and membrane distillation coefficients in direct contact membrane distillation. J Membr Sci 2003;212(1–2):177–93.
[53] Matheswaran M, Kwon TO, Kim JW, Moon SI. Factors affecting flux and water separation performance in air gap membrane distillation. J Ind Eng Chem 2007;13(6):965–70.
[54] Srisurichan S, Jiraratananon R, Fane AG. Mass transfer mechanisms and transport resistances in direct contact membrane distillation process. J Membr Sci 2006;277(1–2):186–94.
[55] Martínez-Díez L, Vázquez-González MI. Temperature and concentration polarization in membrane distillation of aqueous salt solutions. J Membr Sci 1999;156(2):265–73.
[56] Martínez L. Comparison of membrane distillation performance using different feeds. Desalination 2004;168:359–65.
[57] Lawson KW, Lloyd DR. Membrane distillation. J Membr Sci 1997;124(1):1–25.
[58] Chen TC, Ho CD, Yeh HM. Theoretical modeling and experimental analysis of direct contact membrane distillation. J Membr Sci 2009;330(1–2):279–87.
[59] Izquierdo-Gil MA, García-Payo MC, Fernández-Pineda C. Air gap membrane distillation of sucrose aqueous solutions. J Membr Sci 1999;155(2):291–307.